# Radio-Frequency Signal Processing Using Optical Frequency Combs

Mohammed S. Alshaykh, *Student Member, IEEE*, Jason D. McKinney, *Senior Member, IEEE*, and Andrew M. Weiner, *Fellow, IEEE* 

(Invited Paper)

Abstract—Optical frequency combs have established their presence in many fields among which is microwave photonics. Here, we briefly introduce optical frequency comb generators, focusing on high repetition rate combs. Examples of comb-based signal processing are highlighted, including Brillouin mitigation, beamforming, RF-filtering, sub-sampling and RF-channelizers.

*Index Terms*—Integrated optics, Kerr effect, Microwave communication, Microwave photonics, Optical resonators.

#### I. Introduction

NCE their inception, optical frequency combs (OFC) have revolutionized the field of metrology [1] and their impact has extended to numerous fields and applications [2]. Among the fields benefiting from optical frequency combs is microwave or radio-frequency (RF) photonics, where the microwave signal is transferred to optical domain, processed and converted back to electrical domain. For such applications, a free running frequency comb is often sufficient, relieving the need for octave spanning combs and carrier envelope frequency locking (typically done using mode-locked lasers). Furthermore, some signal processing applications particularly benefit from combs with large repetition rate or free spectral range (FSR) that supports large RF-bandwidth operation and paves the way to complex processing through optical pulse shaping. In this paper, we first introduce high FSR (>5 GHz) comb generators that offer moderate bandwidths in the S, C or L bands where optical amplifiers and modulators are widespread. A common feature of the comb sources to be discussed is that they are all generated starting with a continuous wave (CW) laser. We then discuss several examples that illustrate the use of OFCs for RF signal processing, namely: stimulated Brillouin mitigation in long haul analog links, RF filtering, microwave beamforming, sub-sampling and photonic-based RF-channelizers.

Manuscript received September xx, 2019; revised August xx, 2019 and September xx, 2019; accepted September xx, 2019. Date of publication November xx, 2019. This work was supported in part by the U.S. Office of Naval Research under Award N00173-19-1-G900 and by the National Science Foundation under grant 1809784-ECCS. (Corresponding author: M. S. Alshaykh.)

M. S. Alshaykh, and A. M. Weiner are with the School of Electrical and Computer Engineering, Purdue University, West Lafayette, IN 47907, USA and Birck Nanotechnology Center, Purdue University, 1205 West State Street, West Lafayette, Indiana 47907, USA (email: malalsha@purdue.edu; amw@purdue.edu).

J. D. McKinney is with the U.S. Naval Research Laboratory, Washington, DC 20375, USA (e-mail: jason.mckinney@nrl.navy.mil).

### II. GENERATION OF OPTICAL FREQUENCY COMBS

Electro-optic (EO) combs are the most commonly used OFC source in RF-photonics. They have the advantages of reliability, robustness, ease of operation and simple FSR tunability by adjusting the frequency of the driving RF oscillator. Typical commercial LiNbO3 phase modulators have an insertion of loss 2 - 4 dB and support an RF bandwidth of 20 - 40 GHz with a  $V_{\pi}$  of 3 - 4 V at 10 GHz and an RF power handling of 1 W, resulting in  $\sim$  20 spectral lines at -10 dB with a spectral envelope following a Bessel distribution. By cascading intensity (IM) and phase (PM) modulators [3], [4], flat-top combs can be generated, see Fig. 1(c). Further flat comb generation techniques are detailed in [5]. Note that the bandwidth scales linearly with the modulation index or RF-voltage which makes generation of very broad combs challenging. Efforts in integrating such modulators are heavily pursued. Recent advancements in thin-film LN modulators [6] demonstrated impressive improvements in the RF-bandwidth > 100 GHz, reduced loss, high RF-power handling, and a voltage-length product of 2.2 V·cm. In another promising platform for integration, InP, an integrated flat-top comb generator system consisting of an intensity modulator cascaded with 2 PMs generated 28 comb lines. The full system with an onchip laser has a footprint of  $4.5 \times 2.5 \text{ mm}^2$  [7]. Other comb generation techniques, e.g. optically resonant EO architectures, have been demonstrated. For more information the reader should see references [8]-[10].

An outstanding miniaturization of OFC generators is achieved by exploiting cascaded four-wave mixing in high quality factor (Q) integrated nonlinear ring resonators, often referred to as Kerr combs. The resonant enhancement and tight confinement of light along with the right balance between dispersion and loss pave the way to broadband comb generation from a continuous wave pump. The two most common type of resonators are whispering gallery mode resonator (WGM) and on-chip integrated microring resonators. WGM resonators are fabricated using fused silica or crystalline (MgF<sub>2</sub>, CaF<sub>2</sub>) materials and show high Q-factors  $(10^8 - 10^{10})$ . For integrated microcombs, Si<sub>3</sub>N<sub>4</sub> is the most common platform generally offering Qs in the range ca.  $10^5$  -  $10^7$ . Such resonators can generate coherent mode-locked combs of different flavors. In the anomalous dispersion regime, single bright solitons featuring a smooth secant hyperbolic spectral envelope are the sought-after example [11]. In the normal dispersion regime, mode-locked dark pulses with complex spectral envelopes

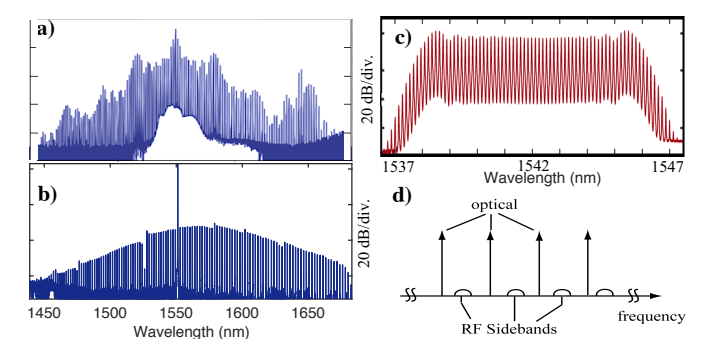


Fig. 1. Spectra of (a) dark pulse [12] and (b) single soliton [16]. c) A 17 GHz EO-comb using an IM and three cascaded PMs [3]. d) The RF signal of interest is impressed onto the optical carrier and replicated at each comb line through modulation.

can be accessed through mode-interaction [12]. Examples of both spectra are shown in Fig. 1(a, b). The pump conversion efficiency of a single bright soliton is on the order 1% or below while dark pulses have been demonstrated with significantly higher conversion efficiencies (10% to 30%) [13]. The FSR of Kerr combs is tightly set by the dimension of the resonator and does not require any external RF drive. The FSRs of demonstrated solitons for WGM are on the order of few to tens of GHz while for microring resonators are typically  $\geq$  80 GHz with the exception of a recent demonstration achieving solitons with FSRs of 10-20 GHz [14]. For a detailed review on Kerr combs and their applications, we refer the reader to [15].

# III. FREQUENCY COMBS FOR RF-SIGNAL PROCESSING

In the intensity modulated direct detection analog link architecture, the optical carrier is modulated by the input RF signal, processed or transmitted in the optical domain, and then downconverted back to the electrical domain via photodetection. The traditional approach uses a CW laser as an optical carrier and has been heavily explored for RF analog signal transmission [17]. Alternatively, an OFC (coherent pulsed optical source) can be used to operate the link as a sampled analog link, where it can be shown that the RF performance follows the traditional link theory [18]. Discretization of the optical carrier in time, however, offers several unique capabilities which are reviewed below. The key concept of OFC-based signal processing is that the RF information is impressed and replicated onto the optical comb as a series of identical sidebands — see Fig. 1(d). The comb line — sideband pairs are employed in different ways depending on the application, e.g., directed onto a single photodetector (RF photonic filtering, sub-sampling) or routed to different detection channels (beamforming, channelization). Fourier domain pulse shaping is frequently used to tailor the power spectrum of the comb (sometimes its spectral phase as well) to the application. If the comb's FSR is equal to or larger than the pulse shaper resolution, the comb's spectral components can be manipulated in a line-by-line fashion. For a detailed tutorial review on pulse shaping, we refer the reader to [19]. In addition, in some cases chromatic dispersion is also used as a tool to impose precise relative delays between the different comb line - sideband pairs.

- 1) Stimulated Brillouin Mitigation: The transmission of analog electrical signals in optical fibers is by far the most studied application of RF photonics. For links exceeding several kilometers, stimulated Brillouin scattering (SBS) limits the optical input launch power imposing detrimental effects on the RF-link metrics. Instead of using a CW laser as the optical carrier, optical pulses (combs) can be used to operate the link as a sampled analog link [18], [20]. Nyquist sampling necessitates that the comb's FSR is larger than or equal to twice the RF bandwidth. By redistributing the average optical power across the comb lines, the SBS power threshold can be increased as long as the FSR exceeds the SBS gain bandwidth and the power spectral density of each line is lower than the CW SBS threshold. Using a 3 GHz EO-comb [21], the SBS threshold was increased by 12.1 dB leading to 10 dB reduction in noise figure (NF) and a 6 dB increase in the spurious free dynamic range (SFDR) compared to a conventional CW link. To scale this to larger RF bandwidths, Kerr combs are wellsuited to generate large FSR combs. In [16], a 73 GHz dark pulse and a 227 GHz soliton were used for SBS mitigation, increasing the threshold by 13.2 dB using a flattened dark pulse. The SFDRs achieved were comparable to those achieved by EO-combs, providing encouraging results for integrated microcombs offering reduced footprint and power consumption. Note that high power in individual comb lines with low relative intensity noise and good optical signal to noise ratio are necessary to achieve reasonable intensity noise and noise figure. Therefore, combs with high optical Kerr comb pump conversion efficiency are preferred.
- 2) RF-Filtering: In OFC-based RF-filtering, the comb is externally modulated by the signal of interest; subsequently, a dispersive medium introduces delays between each comb line. Mathematically, the filter's finite impulse response can be described as  $h(t) = \sum a_n \delta(t - nT)$ , where the tap coefficient  $a_n$  is set by the comb line power, and T is the corresponding tap delay imparted by the dispersive medium. Note that the filter lineshape is the Fourier transform of the impulse response and can be controlled via the weights through pulse shaping. The use of OFCs is advantageous in scaling the number of taps while maintaining stable frequency spacings and low noise starting from a single source. Note that larger FSRs give rise to larger dispersive delays between the taps. A limitation of the tapped delay line configuration using a dispersive element is that the tap coefficients have to be real-valued. To allow complex-valued tap coefficients, the relative phases between the comb lines and their corresponding RF-sidebands must be controlled. Using an EO-comb in an interferometric configuration, where one arm contains a carrier suppressed modulator while the other contains a pulse shaper arbitrarily setting the amplitude or phase of the optical taps, beating on the photodetector transfers the phase information to the RFfilter impulse response [22], [23]. In one example, dynamic filtering of a frequency hopping signal was achieved on a deep submicrosecond scale (Fig. 2(a,b)), demonstrating the versatility of such rapidly tunable filters for ultrabroadband RF spread spectrum applications. Coupled with a balanced detection setup [24], the link performance was pushed to achieve near RF transparency (gain  $\approx 0$  dB) and a noise figure

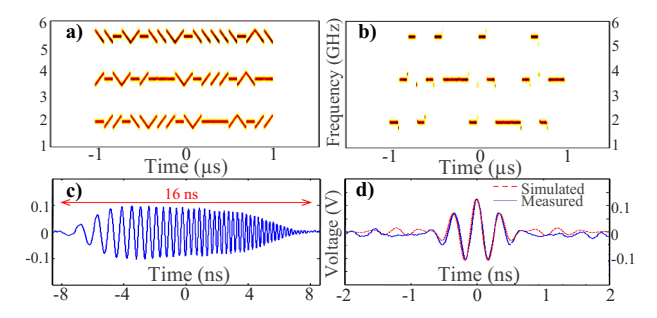


Fig. 2. Rapid dynamic filtering: a) input spectrogram of a frequency-hopping spread spectrum signal and b) spectrogram of the filtered signal. Figures (a,b) adapted from [24]. c) Input chirped pulse (RF bandwidth of 2.7 GHz at -10 dB). d) Compressed pulse after filtering. Figures (c-d) adapted from [23].

~ 7 dB short of the shot noise limit. In another demonstration, arbitrary phase filters were used to compress a wideband (2.7 GHz at -10 dB) RF-waveform chirped to 16 ns as shown in Fig. 2(c-d) [23]. Such filters are essentially analog optical links at their core. Typical out of band rejection values are 20-30 dB; higher rejection (49 to 61 dB) can be achieved through careful apodization of the comb's spectra [22], [25]. Although the bulk of comb-based RF photonic filtering experiments have employed EO combs, proof-of-principle experiments using Kerr combs for filtering [25], [26] and Hilbert transforms [27] have been reported, although with less emphasis so far on RF performance metrics.

3) True-Time delay and beamforming: True time delay (TTD) beamforming is of interest for commercial wireless (e.g., 5 G networks) and defense applications. Instead of mechanically steering the antenna, phased array antennas enable complex beam pattern shaping and steering through the control of the interference and incremental electrical delay between the antennas, respectively [28]. In addition to the hardware reduction offered by OFC-based beamforming, the stable frequency spacing translates to stable delay increments. Here, the OFC passes through a programmable dispersive element adding different delays to different taps or comb lines. The comb lines are then demultiplexed to an array of photodetectors feeding an array of antennas. The far-field pattern is now related to the Fourier-transform of the comb, and different patterns can be programmed by manipulating the comb amplitude through pulse shaping. In addition, by modifying the dispersive element (i.e. the tap delay), beam steering can be achieved. Using a 231 GHz microcomb dark pulse [29], a 21 element TTD beamforming network was demonstrated achieving complex antenna beam shapes and a beam scanning range of  $\pm 60.2^{\circ}$ . Fig. 3 shows a comb spectra shaped to achieve a steerable dark beam (notch) profile, which can be useful for reducing interference from a strong moving emitter in certain applications. A higher number of taps can be achieved using Kerr combs with smaller FSRs, at the expense of a reduced Nyquist zone [30].

For all of the applications discussed so far, shaping of the spectrum may be required. It is therefore critical to consider the comb's original spectral envelope and the effective conversion efficiency after shaping, especially for Kerr combs which can exhibit highly structured combs. For example, in optical communications applications for which a flat spectrum

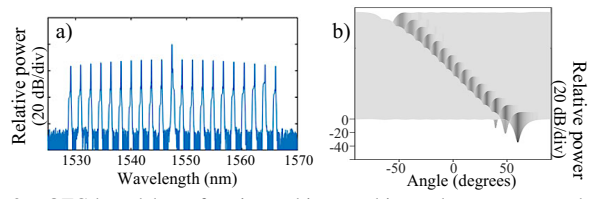


Fig. 3. OFC-based beamforming achieves arbitrary beam patterns through pulse shaping: a) shaped comb spectra with a  $\pi$  phase shift applied to the strong central tap. b) Corresponding steerable dark beam pattern [29].

is desired, dark pulses ideally retain a 2-3 dB advantage compared to solitons after flattening to an equalized spectrum [31].

4) Sub-sampling and RF-Channelizers: Sub-sampling and channelization are two techniques for reducing the RF bandwidth that a digitizer must address at the output of an RF system. Sub-sampling refers to sampling at a rate that intentionally aliases incoming RF signals to a lower intermediate frequency. This operation reduces the RF bandwidth to be digitized to as low as one half the sub-sample rate. Channelization is the selection of a narrow bandwidth around a fixed center frequency prior to downconversion and digitization. In both cases, the RF signals of interest can be digitized at a lower rate utilizing higher-fidelity digitizers than if sampled directly in the RF domain [32].

In sub-sampling, the link is operated as an optically sampled analog link without an electronic preselect filter to limit the input RF bandwidth and photodetected within a bandwidth equal to half the comb's FSR, which is set to be significantly less than the RF bandwidth. These operations lead to aliasing bands that need to be disambiguated. Applying a discrete dither to the sampling pulse train leads to shift in the downcoverted frequency, where the magnitude and direction of the shift are dependant on the signal's original Nyquist zone. Using a 5 GHz EO-comb with a dither of 10 KHz, disambiguation over 16 Nyquist bands (40 GHz) was demonstrated [33]. Instead of an electrically controlled dithering, the nonuniform sampling pulse train can be induced by free space delay modulation irrespective of the original optical comb source [34]. Since the frequency response of a sub-sampled photonic link is the Fourier transform of the sampling pulse intensity at the photodetector, scaling the RF bandwidth requires larger optical bandwidths and compressed pulses. Alternatively, disambiguation can be achieved using dual combs with an offset in the repetition rate, leading to a pair of beatnotes whose spacing and frequency depends on the input signal's Nyquist zone [35], [36]. For EO-combs, the offset in the repetition rate can be straightforwardly controlled by tuning the frequency of RF sinusoid driving the modulators.

Sub-sampling approaches are best suited for sparse RF spectra. For spectrally-dense broadband RF signals for which full disambiguation can be challenging, an RF-channelizer may be a more suitable option. A channelizer uses a filter bank to divide the broadband signal into smaller bandwidth channels that can each be sampled using electronic analog-to-digital (ADC) converters. In OFC-based RF-channelizers, the OFC is externally modulated by the input RF signal creating multiple copies of the signal in the optical domain. Followed by an etalon (periodic filter) with a slightly different FSR, different

sections of RF-signal bandwidth are filtered and subsequently wavelength demultiplexed to an array of photodetectors and ADCs [37]. Recently, a partially coherent 200 GHz Kerr comb was used as a sampling comb followed by a passive 49 GHz microring resonator acting as a periodic filter, with a sliced bandwidth of 1.04 GHz and a potential channelizing bandwidth up to 90 GHz [38]. Alternatively, the modulated comb can be multiplexed and heterodyne detected with a secondary comb whose FSR is mismatched. Through the Vernier effect, different sections of the signal's bandwidth are downconverted to baseband, low pass filtered and sampled. An advantage of this scheme is that it allows coherent reconstruction of the signal [39], [40]. This feature was exploited to allow sub noise detection of fast random events [41].

## IV. CONCLUSION

The highlighted examples demonstrate the versatility of optical frequency combs in RF signal processing. However, for such applications to be useful in real-world scenarios, they must provide RF performance approaching that of their all-electronic counterparts. In particular, the noise figure and spurious-free dynamic range [17] must be suitable for their intended use. It is, therefore, critical to evaluate these optical systems with such conventional RF metrics in parallel to the application-specific measures (e.g., out-of-band rejection for filters, beam-scanning range for beamformers) and potential size-weight-power savings afforded by the use of photonics.

# REFERENCES

- J. L. Hall, "Nobel Lecture: Defining and measuring optical frequencies," *Reviews of Modern Physics*, vol. 78, no. 4, pp. 1279–1295, 2006.
- [2] N. R. Newbury, "Searching for applications with a fine-tooth comb," Nature photonics, vol. 5, no. 4, pp. 186–188, 2011.
- [3] A. J. Metcalf et al., "High-power broadly tunable electrooptic frequency comb generator," *IEEE Journal of Selected Topics in Quantum Electron*ics, vol. 19, no. 6, pp. 231–236, 2013.
- [4] M. A. Soto et al., "Optical sinc-shaped Nyquist pulses of exceptional quality," *Nature communications*, vol. 4, p. 2898, 2013.
- [5] V. Torres-Company and A. M. Weiner, "Optical frequency comb technology for ultra-broadband radio-frequency photonics," *Laser & Photonics Reviews*, vol. 8, no. 3, pp. 368–393, 2014.
- [6] C. Wang et al., "Integrated lithium niobate electro-optic modulators operating at CMOS-compatible voltages," *Nature*, vol. 562, no. 7725, pp. 101–104, 2018.
- [7] N. Andriolli et al., "Photonic integrated fully tunable comb generator cascading optical modulators," *Journal of Lightwave Technology*, vol. 36, no. 23, pp. 5685–5689, 2018.
- [8] M. Kourogi, K. Nakagawa, and M. Ohtsu, "Wide-span optical frequency comb generator for accurate optical frequency difference measurement," *IEEE Journal of Quantum Electronics*, vol. 29, no. 10, pp. 2693–2701, 1993
- [9] Z. Jiang et al., "Spectral line-by-line pulse shaping on an optical frequency comb generator," *IEEE Journal of Quantum Electronics*, vol. 43, no. 12, pp. 1163–1174, 2007.
- [10] M. Zhang *et al.*, "Broadband electro-optic frequency comb generation in a lithium niobate microring resonator," *Nature*, vol. 568, no. 7752, pp. 373–377, 2019.
- [11] T. Herr *et al.*, "Temporal solitons in optical microresonators," *Nature Photonics*, vol. 8, no. 2, pp. 145–152, 2014.
- [12] X. Xue et al., "Mode-locked dark pulse Kerr combs in normal-dispersion microresonators," Nature Photonics, vol. 9, no. 9, pp. 594–600, 2015.
- [13] X. Xue et al., "Microresonator Kerr frequency combs with high conversion efficiency," Laser & Photonics Reviews, vol. 11, no. 1, p. 1600276, 2017.
- [14] J. Liu et al., "Photonic microwave oscillators based on integrated soliton microcombs," arXiv preprint arXiv:1901.10372, 2019.

- [15] T. J. Kippenberg et al., "Dissipative Kerr solitons in optical microresonators," Science, vol. 361, no. 6402, p. eaan8083, 2018.
- [16] M. S. Alshaykh et al., "Kerr combs for stimulated Brillouin scattering mitigation in long-haul analog optical links," *Journal of Lightwave Technology*, 2019, DOI: 10.1109/JLT.2019.2938826.
- [17] V. J. Urick, K. J. Williams, and J. D. McKinney, Fundamentals of microwave photonics. John Wiley & Sons, 2015.
- [18] J. D. McKinney and K. J. Williams, "Sampled analog optical links," IEEE Transactions on Microwave Theory and Techniques, vol. 57, no. 8, pp. 2093–2099, 2009.
- [19] A. M. Weiner, "Ultrafast optical pulse shaping: A tutorial review," *Optics Communications*, vol. 284, no. 15, pp. 3669–3692, 2011.
- [20] V. J. Urick et al., "Long-haul analog photonics," Journal of Lightwave Technology, vol. 29, no. 8, pp. 1182–1205, 2011.
- [21] J. D. McKinney, V. J. Urick, and J. Briguglio, "Optical comb sources for high dynamic-range single-span long-haul analog optical links," *IEEE Transactions on Microwave Theory and Techniques*, vol. 59, no. 12, pp. 3249–3257, 2011.
- [22] V. Supradeepa *et al.*, "Comb-based radiofrequency photonic filters with rapid tunability and high selectivity," *Nature Photonics*, vol. 6, no. 3, pp. 186–194, 2012.
- [23] M. Song et al., "Compression of ultra-long microwave pulses using programmable microwave photonic phase filtering with >100 complexcoefficient taps," Optics express, vol. 22, no. 6, pp. 6329–6338, 2014.
- [24] H.-J. Kim, D. E. Leaird, and A. M. Weiner, "Rapidly tunable dual-comb RF photonic filter for ultrabroadband RF spread spectrum applications," *IEEE Transactions on Microwave Theory and Techniques*, vol. 64, no. 10, pp. 3351–3362, 2016.
- [25] X. Xu et al., "Advanced adaptive photonic RF filters with 80 taps based on an integrated optical micro-comb source," *Journal of Lightwave Technology*, vol. 37, no. 4, pp. 1288–1295, 2019.
- [26] X. Xue et al., "Programmable single-bandpass photonic RF filter based on Kerr comb from a microring," Journal of Lightwave Technology, vol. 32, no. 20, pp. 3557–3565, 2014.
- [27] T. G. Nguyen et al., "Integrated frequency comb source based Hilbert transformer for wideband microwave photonic phase analysis," Optics express, vol. 23, no. 17, pp. 22 087–22 097, 2015.
- [28] R. Rotman, M. Tur, and L. Yaron, "True time delay in phased arrays," Proceedings of the IEEE, vol. 104, no. 3, pp. 504–518, 2016.
- [29] X. Xue et al., "Microcomb-based true-time-delay network for microwave beamforming with arbitrary beam pattern control," *Journal of Lightwave Technology*, vol. 36, no. 12, pp. 2312–2321, 2018.
- [30] X. Xu et al., "Photonic microwave true time delays for phased array antennas using a 49 GHz FSR integrated optical micro-comb source," Photonics Research, vol. 6, no. 5, pp. B30–B36, 2018.
- [31] Ó. B. Helgason et al., "Superchannel engineering of microcombs for optical communications," JOSA B, vol. 36, no. 8, pp. 2013–2022, 2019.
- [32] R. H. Walden, "Analog-to-digital converter survey and analysis," *IEEE Journal on selected areas in communications*, vol. 17, no. 4, pp. 539–550, 1999.
- [33] S. R. Harmon and J. D. Mckinney, "Precision broadband RF signal recovery in subsampled analog optical links," *IEEE Photonics Technology Letters*, vol. 27, no. 6, pp. 620–623, 2014.
- [34] R. T. Schermer and J. D. McKinney, "Non-uniform sub-Nyquist optical sampling by acousto-optic delay modulation," *Journal of Lightwave Technology*, vol. 36, no. 21, pp. 5058–5066, 2018.
- [35] A. Klee, C. Middleton, and R. DeSalvo, "Dual-comb spectrometer for fast wideband RF spectral analysis," in 2017 IEEE Photonics Conference (IPC). IEEE, 2017, pp. 379–380.
- [36] M. S. Alshaykh et al., "Rapid wideband RF subsampling and disambiguation using dual combs," in CLEO: Science and Innovations. Optical Society of America, 2019, pp. SF2N-8.
- [37] X. Xie et al., "Broadband photonic radio-frequency channelization based on a 39-GHz optical frequency comb," *IEEE Photonics Technology Letters*, vol. 24, no. 8, pp. 661–663, 2012.
- [38] X. Xu et al., "Broadband RF channelizer based on an integrated optical frequency Kerr comb source," *Journal of Lightwave Technology*, vol. 36, no. 19, pp. 4519–4526, 2018.
- [39] X. Xie et al., "Broadband photonic RF channelization based on coherent optical frequency combs and I/Q demodulators," IEEE Photonics Journal, vol. 4, no. 4, pp. 1196–1202, 2012.
- [40] A. Wiberg et al., "Coherent filterless wideband microwave/millimeterwave channelizer based on broadband parametric mixers," Journal of Lightwave Technology, vol. 32, no. 20, pp. 3609–3617, 2014.
- [41] V. Ataie et al., "Subnoise detection of a fast random event," Science, vol. 350, no. 6266, pp. 1343–1346, 2015.